Jurnal Teknologi

Full paper

Asymmetric Polysulfone-Cloisite 15A® Nanocomposite Membrane for Gas Separation

A. K. Zulhairun, A. F. Ismail*, A. Mustafaa

Advanced Membrane Technology Research Centre (AMTEC), Universiti Teknologi Malaysia, 81310 UTM Johor Bahru, Johor, Malaysia

*Corresponding author: afauzi@utm.my

Article history

Received :15 September 2013
Received in revised form :
17 November 2013
Accepted :15 January 2014

Graphical abstract

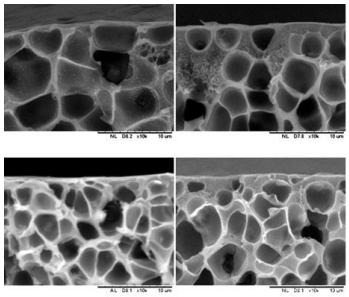

Abstract

Defect-free asymmetric Polysulfone (PSF)-Cloisite 15A® nanocomposite membrane was fabricated with the intention to investigate the gas permeation behavior of the resulting material combination. Various weights of Cloisite 15A® organoclay were added into PSF matrices by solution intercalation method assisted by sonication dispersion. The gas permeation properties of the PSF-Cloisite 15A® nanocomposite membranes were evaluated by pure gases: nitrogen, methane, and carbon dioxide. The distribution of Cloisite 15A® particles in PSF matrices was analyzed by SEM. The gas flux of the PSF-Cloisite 15A® nanocomposite membranes declined as the Cloisite 15A® weight loading increased. The CO_2/CH_4 and CO_2/N_2 pure gas selectivity of PSF nanocomposite with 0.5 wt. % of Cloisite 15A® loading exceeded that of neat PSF membrane. The decrease in flux followed by the increase in pure gas selectivity was related to the way in which the clay layers were dispersed in the PSF matrices. Considerable improvement in CO_2 selectivity was attainable even by incorporating low amount of such layered structure nanoparticle which can be attractive in producing robust materials for CO_2-removal membranes from CO_2-containing gas streams such as post-combustion and natural gas streams.

Keywords: Nanocomposite membrane; layered silicate; clay minerals; exfoliation; gas separation

1.0 INTRODUCTION

In pursuing robust and efficient membrane material for industrial gas separation application, the development of mixed matrix or nanocomposite membranes has become one of major studies in academic and industrial research and development. Recent progress in advanced material development have shown growing interest in investigation on layer structure inorganic particles such as AMH-3 [1, 2], UZAR-S1 [3], JDF-L1 [3], AlPO [4], Nu-6 (2) [5] zeolite, etcetera. These materials possess very high aspect ratio, thus a high surface area of polymer/filler contact. The unique properties of these fillers have shown significant changes in membrane characteristics with the presence of only a small amount of these inorganic materials[1-5].

Montmorillonites clay mineral, is an example of naturally occurring inorganic particle, having a sheet-type or platy structure. This type of particle has not yet received large attention in mixed matrix membrane development for gas separation purposes, even though this filler has been recognized as one of the most prominent filler in nanocomposite industries [6, 7]. One of the most unique features of this naturally occurring mineral is the capability of the silicate layers to be delaminated into individual nanoplatelets of very high aspect ratio in a polar matrix, which is not exhibited by other conventional fillers. This nanoscale morphology has been exploited in polymer nanocomposite industries in order to improve the physical-chemical properties of polymeric materials.

To date, experimental data on clay-polymer hybrid membrane for gas separation purpose is still diminutive in contrast to other filler-polymer combinations. Cloisite 15A® (C15A) is an organically modified montmorillonite was selected in the present research to fabricate high-performance gas separation nanocomposite membranes. As for the continuous phase, polysulfone (PSF) is a fine choice of membrane material for gas separation due to a practical combination between its permeability and selectivity in addition to its good mechanical and thermal properties as well as easy processability. It should also be noted that, most of the prior studies mainly focused on characterizing dense clay-polymer hybrid films. To our knowledge, there is no documentation on the use of C15A clay mineral incorporated into polysulfone matrix for the production of asymmetric mixed matrix membrane for gas separation. In this work we will examine the impact of the C15A loading on the PSF nanocomposite physico-chemical, morphology and the gas transport properties.

2.0 EXPERIMENTAL

2.1 Materials

Polysulfone (PSF Udel-P3500) as polymer matrix phase was supplied by Amoco Chemicals. N,N-dimethylacetamide (DMAc) and tetrahydrofuran (THF) were supplied by Merck and from QReC respectively. Ethanol, supplied by Merk, was used as a non-solvent additive. The inorganic filler, montmorillonite organoclay, known with the trade name Cloisite® 15A hereafter referred as C15A, was purchased from Southern Clay Products, Inc., USA. PSF pellet and C15A powder were preconditioned in a vacuum oven at 80°C for at least 72 h to remove trapped moisture, whereas other organic chemicals obtained in reagent grade purities were used as received.

2.2 Methods

The dope solutions in this study were formulated to consist of 30 wt.% PSF, 35 wt.% DMAc (non-volatile solvent), 30 wt.% THF (volatile solvent) and 5 wt.% ethanol (non-solvent), without inclusing C15A, while the amount of C15A incorporated in the dope solution was from 0.5 to 3.0 wt.% of PSF.

The details of the dope preparation method are as follows: Firstly, DMAc and THF are mixed in a 100 ml glass bottle and subjected to sonication in ultrasonication bath. The predetermined amount of clay powder was poured into the mixed solvents (DMAc and THF) whilst sonication took place. Sonication on the filler-polymer suspension was conducted for 90 minutes at 60°C. The filler was then subjected to priming for a 4 h period upon the addition of 1/10 of the total PSF to the suspension in order to ensure optimum wetting of C15A particles. Finally, the remaining PSF was gradually added to the solution and stirred until complete dissolution of the polymer was achieved. The non-solvent, ethanol was the last component to be added to the solution in completion of the aforementioned formulation. The dope was finally degassed prior to membrane fabrication.

Asymmetric flat sheet membranes were prepared according to the dry/wet phase inversion technique. The dope solution was poured onto a clean, flat glass plate and then immediately spread to a uniform thickness of approximately 200 μm. The nascent membrane film was allowed to undergo free standing evaporation for 100 s in ambient atmosphere and subsequently immersed in the water. The membranes were kept immersed in the aqueous bath for 1 day, followed by a solvent-exchange post treatment process in which the membranes were immersed in methanol and *n*-hexane, for 2 hours respectively. Afterwards, the membranes were left to dry for 24 hours at room temperature before further tests and characterizations.

The gas permeation experiment on the asymmetric membranes was conducted using pure N_2, CH_4 and CO_2 gases with purity of 99.99%. A circular membrane disc with an effective permeation area of 13.5 cm^2 was mounted in a stainless steel permeation cell of a constant pressure system. The pressure-normalized fluxes of the membranes are measured at 25°C at 5 bar gauge pressure. A soap bubble flow meter was attached to the permeate side of the cell to measure the rate at which the gas permeates across the membrane. The permeance was calculated by the equation:

$$\frac{P_i}{l} = \frac{Q}{A\Delta P}\frac{273.15}{T} \quad (1)$$

where P_i/l is the gas permeance of a membrane in GPU (1 GPU = 1×10^{-6} cm^3 (STP) /cm^2.s.cmHg), i represents the penetrating gas i, Q is the volumetric flow rate of gas permeated through the membrane (cm^3/s, STP), A the effective membrane area (cm^2), and ΔP is the pressure difference across the membrane (cmHg). The ideal selectivity was simply determined as the permeability ratio of the fast gas to slow gas:

$$\alpha_{i/j} = \frac{P_i / l}{P_j / l} \quad (2)$$

where $\alpha_{i/j}$ is the selectivity of gas penetrant i to gas penetrant j, P_i/l and P_j/l are the permeance of gas penetrant i and j, respectively.

The morphology of the prepared nanocomposite membranes and treated and untreated organoclays were scrutinized by scanning electron microscopic (SEM), made by TM3000 Tabletop Microscope. The membrane samples were frozen and fractured inside liquid nitrogen to form smooth break of the membrane cross-section. The fractured samples were mounted on carbon tape masking on stainless steel stand and subsequently sputter-coated with thin layer of gold prior to SEM analysis.

3.0 RESULTS AND DISCUSSION

Figure 1 shows the differences between the as-received C15A particle with the post-sonicated C15A particle under SEM observation. From the image, the as-received C15A powder indeed exhibits the structure of layered particle but is lumped together, forming bulky micron-sized aggregates. Whereas, we can clearly observe the silicate layers become swell after the sonication process. On top of that, the clay particles are more segregated and smaller in size.

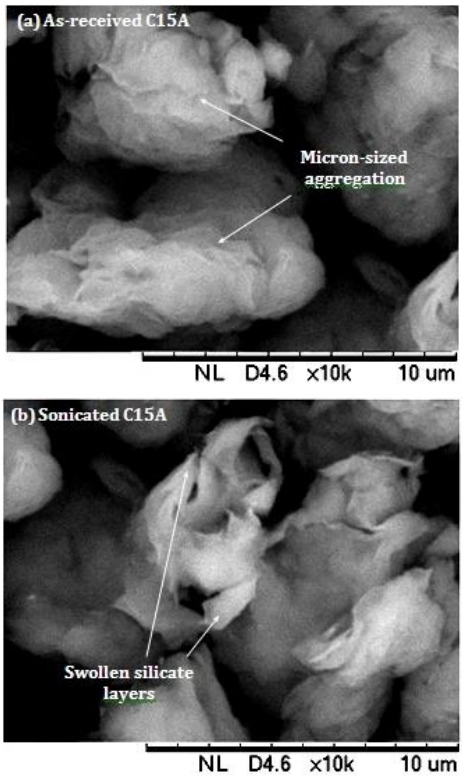

Figure 2 SEM image of the (a) as-received C15A, and the (b) swollen-induced C15A by sonication-dispersion technique

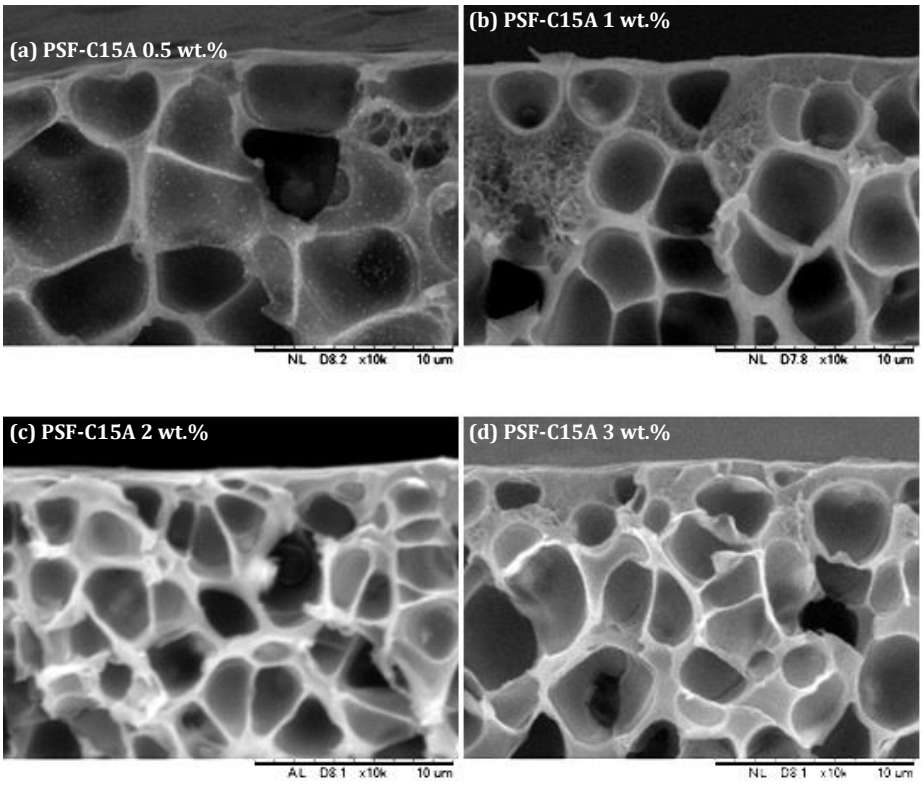

Figure 2 SEM cross-section image of (a) PSF-C15A 0.5 wt.%, (b) PSF-C15A 1 wt.%, (c) PSF-C15A 2 wt.% and (d) PSF-C15A 3 wt.% nanocomposite membranes

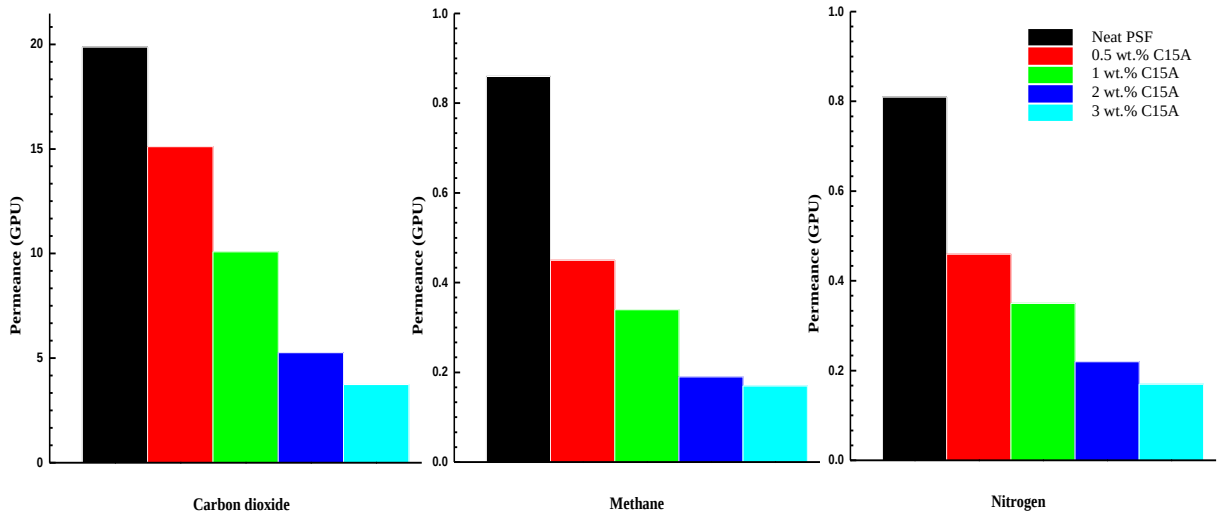

Figure 3 The comparison of gas permeance for neat PSF and PSF-C15A nanocomposite membranes with different C15A loadings

Cross sections of nanocomposite membranes prepared with various clay loadings were observed by SEM to verify the homogeneity and the intimate contact of the layered silicate dispersion as well as the overall morphology of the membranes. Figure 2(a)-(d) illustrates the SEM cross-section images of PSF-C15A0.5, PSF-C15A1, PSF-C15A2 and PSF-C15A3 nanocomposite membranes, respectively. As expected, integrally skinned asymmetric membranes were successfully produced by solution casting, via dry/wet non-solvent induced phase separation. All membranes exhibit a morphology of integrally skinned asymmetric membrane formed on a porous sub-layer containing "tear drop" macro-voids that, presumably give negligible effect on separation.

From the SEM cross-sectional image, we were having difficulties in locating the layered silicate particles throughout the matrix. This suggests that the clay particles have been succe ssfully dispersed in the matrix to molecular level and intimately assimilated with the PSF matrix. Good adherance between this filler and PSF matrix is well anticipated owing to the

modification of the surface chemistry of this filler by quaternary ammonium dimethyl-dihydrogenated tallow (DMDHT) [8, 9].

Table 1 Average permeance and selectivity values for CO_2/CH_4 and CO_2/N_2 gas pairs at 5 bar, 25°C

Sample	Permeance ($P_{i/j}/l$), GPU[a]			Selectivity ($\alpha_{i/j}$)	
	N_2	CH_4	CO_2	CO_2/CH_4	CO_2/N_2
PSF Neat	0.81	0.86	19.88	23.12	24.54
PSF-C15A 0.5 wt.%	0.46	0.45	15.11	31.50	32.85
PSF-C15A 1.0 wt.%	0.35	0.34	10.09	29.58	29.18
PSF-C15A 2.0 wt.%	0.22	0.19	5.27	27.23	24.49
PSF-C15A 3.0 wt.%	0.17	0.17	3.75	21.85	22.06

[a] 1 GPU = 1×10^{-6} cm^3 (STP)/cm

The effect of C15A loading on the gas permeation behavior was investigated by a variable volume constant pressure method, using pure N_2, CH_4, and CO_2 at feed pressure 5 bar gauge, conducted at room temperature. In this study, the membranes fabricated were essentially defect-free, since no coating treatment was needed to achieve the intrinsic selectivity of the pure polymer. This can be accredited to well-formulated dope composition and the control of membrane fabrication conditions. Figure 3 exhibits the gas permeance of neat PSF and nanocomposite membranes with different C15A loadings. It can be clearly seen that the permeance of PSF-C15A nanocomposite membranes from all loadings are lower than that of neat PSF membrane. The decline in gas permeation flux was about 40 to 80% with increasing C15A loading from 0.5 wt.% to 3 wt.%. Clearly, the decrease in gas permeation flux is mainly due to the exfoliation of impermeable clay nanoparticles in the membrane matrix. In principle, since the clay layers not possessing any accessible pores, the gas molecules were forced to flow along tortuous pathway across the clay-filled polymer matrix [10].

Furthermore, additional contributing factors which lead to flux reduction was most probably due to the high aspect ratio of the exfoliated silicate layers and the nature of layered silicate clays, which might have been horizontally aligned to the matrix plane contributing to high barrier towards molecular diffusion [11]. Due to the high contact surface area as well as good interactions established between the inorganic phase with the polymer matrix, polymer chain rigidity may also be enhanced. This in turn affects the overall molecular vibration of polymer chain at the polymer-filler interface which may also result in declining gas flux through the nanocomposite membranes.

From Figure 3 we also realize that the diffusion-mitigating effect impinged the permeation of all gases tested, but pose rather greater impact on larger gas molecules *i.e.* CH_4 and N_2. Therefore, the drastic reduction in CH_4 and N_2 permeance resulted in enhancement of CO_2/N_2 and CO_2/CH_4 ideal selectivity compared to the unfilled PSF membrane as presented in Table 1. Selectivity enhancement accredited by the increase in diffusivity difference among the penetrating molecules has also been encountered in the literature as a result of incorporating high aspect ratio inorganic particles [12-14].

Figure 4 is drawn to illustrate the selective-diffusion scheme of gas molecules through polymer matrix filled with highly dispersed, ideally exfoliated, and oriented clay layers.

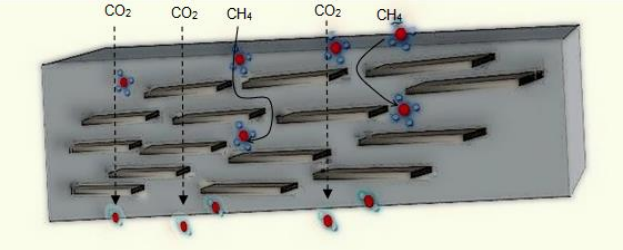

Figure 4 Gas permeation mechanism through highly oriented layered silicate-polymer system

In the case where CO_2/CH_4 mixture to be separated, the more condensable gas, namely CO_2, diffuses through the clay-filled matrix relatively more freely compared to less condensable, larger kinetic diameter molecules [15]. Selectivity of small gas over large gas mixtures such as H_2/CH_4 may be greatly enhanced in such mixed-matrix system incorporating perpendicularly aligned, high aspect ratio layer structure filler as reported in the literature [11, 14, 16]. However, the increase in selectivity seem to be compensated by inevitable loss in gas permeation flux, following the typical performance trade-off. Proper tuning of the layered silicate loading, may lead to achieving the superior selectivity, while maintaining its attractive permeance for feasible large scale implementation of this so-called mixed-matrix layered silicate nanocomposite membrane.

4.0 CONCLUSION

On contrary to typical investigation on symmetrically dense membrane, flat asymmetric mixed-matrix membrane was the prime focus of this study. This study reports successful formation of defect-free asymmetric nanocomposite membrane incorporating layered structure organoclay, Cloisite 15A® in polysulfone matrix for gas separation application. Considerable decrease in gas permeation flux was observed with increasing clay content. The reduction in gas flux was believed to be attributed by the exfoliation of the impermeable clay layers in the membrane matrix which forcing the molecules to travel along tortuous diffusion pathway to permeate across the clay-filled polymer matrix. The loss in flux was rewarded with over 30% improvement on CO_2/CH_4 and CO_2/N_2 selectivity, even with very low amount of filler incorporated. Selectivity enhancement was accredited by the increase in diffusivity difference due to the presence of highly oriented clay lamellar in the membrane matrix.

Acknowledgement

The authors would like to thank Ministry of Education Malaysia and Universiti Teknologi Malaysia (UTM) for funding this research with the grant number Q.J130000.2542.04H71.

References

[1] S. Choi, J. Coronas, Z. Lai, D. Yust, F. Onorato, M. Tsapatsis. 2008. *J. Membr. Sci*. 145: 152.
[2] W. Kim, J. S. Lee, D. G. Bucknall, W. J. Koros, S. Nair. 2013. *J. Membr. Sci*. 129: 136.
[3] C. Rubio, C. Casado, P. Gorgojo, F. Etayo, S. Uriel, C. Tellez, J. Coronas. 2010. *Eur. J. Inorg. Chem.* 159: 163.
[4] C. Wang, W. Hua, Y. Yue, Z. Gao. 2007. *Microporous and Mesoporous Materials.* 149: 155.
[5] P. Gorgojo, S. Uriel, C. Téllez, J. Coronas. 2008. *Microporous and Mesoporous Materials*. 85: 92.
[6] A. Okada, A. Usuki. 1995. *Materials Science and Engineering*. 109: 115.
[7] F. Bergaya. 2008. *Microporous and Mesoporous Materials.* 141: 148.
[8] J. Jaafar, A. F. Ismail, T. Matsuura, K. Nagai. 2011. *J. Mem. Sci.* 202: 211.
[9] S. A. Hashemifard, A. F. Ismail T. Matsuura. 2011. *Chem. Eng. J*. 316: 325.
[10] G. Choudalakis, A. D. Gotsis. 2009. *Eur. Polym. J.* 967: 984.
[11] S. Castarlenas, P. Gorgojo, C. Casado-Coterillo, S. Masheshwari, M. Tsapatsis, C. Tellez, J. Coronas. 2013. *Indus. Eng. Chem. Res.* 1901: 1907.
[12] A. Galve, D. Sieffert, E. Vispe, C. Tellez, J. Coronas, C. Staudt. 2011. *J. Membr. Sci.* 131: 140.
[13] M. A. Aroon, A. F. Ismail, T. Matsuura. 2013. *Sep. Pur. Tech.* 39: 50.
[14] B. R. Vaughan, E. Marand. 2008. *J. Membr. Sci.* 197: 207.
[15] H. K. Jeong, W. Krych, H. Ramanan, S. Nair, E. Marand, M. Tsapatsis. 2004. *Chem. Mater*. 3838: 3845.
[16] A. Galve, D. Sieffert, C. Staudt, M. Ferrando, C. Guell, C. Tellez, J. Coronas. 2013. *J. Membr. Sci.* 163: 170.